

FIG. 4 The difference between the observed and modelled global mean temperature for the five cases cited in Table 1. The cases which include greenhouse forcing, cases 3, 4 and 5, result in lower error variance than the cases based on solar forcing alone, cases 1 and 2. On the basis of error variance, case 4 is the most plausible simulation although  $\beta$  in this case is considerably higher than suggested by recent satellite data. Not surprisingly, fluctuations on interannual to decadal timescales are present in the residuals in each case. None of the simulations adequately accounts for the warmth of the years around 1940 and the trends in adjacent decades. This discrepancy may be the result of the influence of other forcing agents, internal climate variability and/or other factors neglected in these simulations.

and determine the climate sensitivity, other factors, such as internally generated climate variability<sup>21</sup> and the effect of additional external forcing agents<sup>1-3</sup>, would have to be taken into account<sup>22</sup>.

Our results do indicate that, since the mid-nineteenth century, the influence of the enhanced greenhouse effect on global mean temperature has almost certainly dominated over the direct influence of solar variability. For solar variability to have been an important contributing factor, past low-frequency variations in solar irradiance would have to have been far greater than recent satellite studies indicate. There is no firm evidence to support this contention. Compared to the well established observational and theoretical basis for the influence of increased greenhouse forcing, the case for a solar effect on recent changes in global climate is speculative in the extreme. □

Received 21 May; accepted 17 August 1990

1. Hansen, J. et al. *Science* **213**, 957-966 (1981).
2. Gilliland, R. L. *Clim. Change* **4**, 111-131 (1982).
3. Gilliland, R. L. & Schneider, S. H. *Nature* **310**, 38-41 (1984).
4. Reid, G. C. *Nature* **329**, 142-143 (1987).
5. Seitz, F., Jastrow, R. & Nierenberg, W. A. *Scientific Perspectives on the Greenhouse Problem* (George C. Marshall Institute, Washington, DC, 1989).
6. Hoffert, M. I., Callegari, A. J. & Hsieh, C.-T. *J. geophys. Res.* **85**, 6667-6679 (1980).
7. Hoffert, M. I. & Flannery, B. P. in *Projecting the Climatic Effects of Increasing Carbon Dioxide, DOE/ER-0237* (eds MacCracken, M. C. & Luther, F. M.) 149-190 (US Department of Energy, Washington, DC, 1985).
8. Folland, C. K., Parker, D. E. & Kates, F. E. *Nature* **310**, 670-673 (1984).
9. Wigley, T. M. L. & Raper, S. C. B. *Nature* **330**, 127-131 (1987).
10. Hansen, J. & Lacis, A. *Nature* **346**, 713-719 (1990).
11. Lean, J. & Foukal, P. *Science* **240**, 906-908 (1988).

12. Foukal, P. & Lean, J. *Science* **247**, 556-558 (1990).
13. Wigley, T. M. L. & Raper, S. C. B. *Geophys. Res. Lett.* (in the press).
14. Wigley, T. M. L. & Kelly, P. M. *Phil. Trans. R. Soc. A* **330**, 547-560 (1990).
15. Intergovernmental Panel on Climate Change *Scientific Assessment of Climate Change, Working Group 1 Report* (Intergovernmental Panel on Climate Change/World Meteorological Organization/United Nations Environment Programme, Geneva, 1990).
16. Gage, K. & Reid, G. C. *Geophys. Res. Lett.* **8**, 187-190 (1981).
17. Wigley, T. M. L., Angell, J. K. & Jones, P. D. in *Detecting the Climatic Effects of Increasing Carbon Dioxide, DOE/ER-0235* (eds MacCracken, M. C. & Luther, F. M.) 55-90 (US Department of Energy, Washington, DC, 1985).
18. Jones, P. D., Wigley, T. M. L. & Wright, P. B. *Nature* **322**, 430-434 (1986).
19. Jones, P. D. et al. *J. Clim. appl. Met.* **25**, 161-179 (1986).
20. Jones, P. D., Raper, S. C. B. & Wigley, T. M. L. *J. Clim. appl. Met.* **25**, 1213-1230 (1986).
21. Wigley, T. M. L. & Raper, S. C. B. *Nature* **344**, 324-327 (1990).
22. Wigley, T. M. L. & Barnett, T. P. in *Scientific Assessment of Climate Change, Working Group 1 Report* (Intergovernmental Panel on Climate Change/World Meteorological Organization/United Nations Environment Programme, Geneva, 1990).

ACKNOWLEDGEMENTS. This work was supported by the US Department of Energy, Carbon Dioxide Research Division.

## A carbon isotope record of CO<sub>2</sub> levels during the late Quaternary

John P. Jasper & J. M. Hayes

Biogeochemical Laboratories, Departments of Geological Sciences and of Chemistry, Indiana University, Bloomington, Indiana 47405-5101, USA

ANALYSES of gases trapped in continental ice sheets have shown that the concentration of CO<sub>2</sub> in the Earth's early atmosphere increased from 180 to 280 p.p.m. during the most recent glacial-interglacial transition<sup>1</sup>. This change must have been driven by an increase in the concentration of CO<sub>2</sub> dissolved in the mixed layer of the ocean<sup>2</sup>. Biochemical and physiological factors associated with photosynthetic carbon fixation in this layer should lead to a relationship between concentrations of dissolved CO<sub>2</sub> and the carbon isotopic composition of phytoplanktonic organic material<sup>3</sup>, such that increased atmospheric CO<sub>2</sub> should enhance the difference in <sup>13</sup>C content between dissolved inorganic carbon and organic products of photosynthesis. Here we show that a signal related to atmospheric CO<sub>2</sub> levels can be seen in the isotope record of a hemipelagic sediment core, which we can correlate with the CO<sub>2</sub> record of the Vostok ice core. Calibration of the relationship between isotope fractionation and CO<sub>2</sub> levels should permit the extrapolation of CO<sub>2</sub> records to times earlier than those for which ice-core records are available.

Popp and coworkers<sup>3</sup> have suggested a relationship between carbon isotope fractionation and dissolved CO<sub>2</sub> of the form

$$\epsilon_P = a \log c + b \quad (1)$$

where  $\epsilon_P$  is the isotope effect (‰) associated with photosynthetic fixation of carbon,  $c$  is the concentration of dissolved CO<sub>2</sub> (μM), and  $a$  and  $b$  are constants. In an open system, the isotope fractionation between substrate and product is numerically equal to  $\epsilon$ . The functional form of equation (1) seems to be representative of biologically mediated  $\epsilon_P$ -CO<sub>2</sub> relationships, but the dependence of  $a$  and  $b$  on physiological, ecological and environmental factors is just beginning to be characterized<sup>3-5</sup>. Here, this problem is explored by comparison of historical records of  $\epsilon_P$  and  $p_{CO_2}$ .

To determine values of  $\epsilon_P$  in ancient environments, we must reconstruct the isotopic compositions of dissolved CO<sub>2</sub> and phytoplanktonic biomass. In surface sea water, dissolved CO<sub>2</sub> is depleted in <sup>13</sup>C relative to total dissolved inorganic carbon (DIC) by 8.8‰ ( $T = 24^\circ\text{C}$ ,  $\text{pH} = 8.2$ ). In turn, calcite tests produced by the planktonic foraminifera *Globigerinoides ruber* are depleted in <sup>13</sup>C relative to DIC by an average of 0.5‰<sup>6,7</sup>. Determination of the isotopic composition of these microfossils ( $\delta_{G. ruber}$ ) therefore allows estimation of the <sup>13</sup>C content of ancient dissolved CO<sub>2</sub>. Although all sedimentary organic carbon is ultimately of photosynthetic origin, most of it has been reworked and isotopically fractionated during its passage through the marine food chain<sup>8</sup>. To construct a record of isotopic

compositions of microalgae, it is therefore necessary to isolate specific molecular products of these organisms<sup>3</sup>. We have used isotope-ratio-monitoring gas chromatography/mass spectroscopy techniques<sup>9</sup> to determine isotopic compositions of  $C_{37}$  alkenones ( $\delta_{37:2}$ ), which can be readily isolated from many sediments<sup>10</sup>. These molecules derive specifically from prymnesiophyte algae (such as coccolithophorids)<sup>11</sup>. Analyses of laboratory cultures show that the alkenones are depleted in  $^{13}C$  by 3.8‰ relative to total algal cell material. Values for  $\epsilon_P$  are determined from

$$\epsilon_P = 1,000[(\delta_P + 1,000)/(\delta_d + 1,000) - 1] \quad (2)$$

where  $\delta_P$  (‰) ( $=\delta_{37:2} + 3.8$ ) and  $\delta_d$  (‰) ( $=\delta_{G.ruber} - 8.3$ ) are the carbon isotopic compositions of prymnesiophyte biomass and dissolved  $CO_2$ , respectively.

We have examined samples from a sediment core obtained at Deep Sea Drilling Project site 619, in the Pigmy Basin, northern Gulf of Mexico<sup>12,13</sup>. Bottom waters in the basin are oxic and of normal salinity<sup>13</sup>. Sedimentation rates determined for oxygen isotope substages 1 to 5b<sup>14,15</sup> varied from 71 to 92 cm kyr<sup>-1</sup> during interglacial periods, and from 230 to 300 cm kyr<sup>-1</sup> during glacial periods, presumably owing to

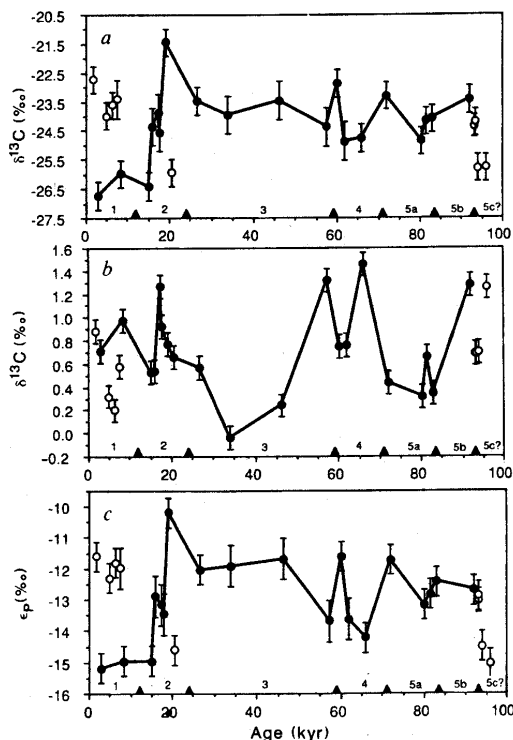


FIG. 1 a, Carbon isotopic compositions of samples of heptatriacontatriene-2-one<sup>29,30</sup> extracted from intervals of DSDP Hole 619<sup>10</sup> (displaced sediments are represented by open circles). ( $\delta^{13}C(\text{‰}) = 1,000[(R_{\text{sample}}/R_{\text{PDB}}) - 1]$ , where  $R = {}^{13}C/{}^{12}C$  and  $R_{\text{PDB}} = 0.0112372$ ). Ages were assigned from boundaries of the oxygen isotope stages<sup>14</sup> and are compatible with three phytoplanktonic foraminiferal boundaries<sup>19,31</sup>, a volcanic ash layer<sup>32</sup>, and an accelerator  $\Delta^{14}C$  date (for details see ref. 15). b, Carbon isotopic compositions of calcite tests of *G. ruber*. c, Isotope fractionation between  $C_{37}$  alkenones and *G. ruber* calcite expressed in terms of the fractionation factor  $\epsilon_P$  (see equation (2)).

increased erosion of continental material during times of falling sea level and at low sea-level stands<sup>14,16,17</sup>. Individual samples spanned between 17 and 70 years and were also mixed by bioturbation, thus averaging effects of seasonal variations in  $p_{CO_2}$ .

The  $\delta_{37:2}$ ,  $\delta_{G.ruber}$  and  $\epsilon_P$  records are shown in Fig. 1. The data points marked by open circles are believed to derive from turbidity flows or sediment slumps, common to the northern Gulf of Mexico<sup>18</sup>. They have been recognized on the basis of discontinuities in the records of  $^{13}C$  in total organic carbon<sup>15</sup>,  $^{18}O$  in carbonates<sup>14</sup>, and  $U_{37}^K$  ( $C_{37:2}/(C_{37:2} + C_{37:3})$ ), where  $C_{37:2}$  and  $C_{37:3}$  are the concentrations of the di- and tri-unsaturated alkenones; see ref. 10). In spite of the 2,300-m depth of the basin, the deepest portion of the core (termed isotope substage '5c') contained shallow-water microfossils and quartz sand, indicating the presence of displaced sediments<sup>14,19</sup>.

The chronology of the Vostok ice core is based on a two-dimensional snow accumulation and ice-flow model<sup>20</sup>, whereas that of marine sediments is commonly based on the oxygen isotope record in carbonate microfossils. Precise correlation ( $\pm 2$  kyr) between ice and sediment cores can be difficult. Moreover, whereas  $p_{CO_2}$  values have been directly recorded in the ice by physical entrapment of an air sample, the recording of  $CO_2$  levels in sediment cores is indirect. Variable factors of two kinds are involved. First, the concentration of  $CO_2$  dissolved in the photic zone may not be in equilibrium with atmospheric  $p_{CO_2}$  (ref. 21). Second, relationships between  $\epsilon_P$  and  $c$  are only now being quantified. We will consider these points separately.

Concentrations of dissolved  $CO_2$  in surface waters of the Gulf of Mexico 2–100 kyr ago are not directly known. If we use the Vostok record of atmospheric  $p_{CO_2}$  values<sup>1</sup> to estimate values of  $c$  and assume equilibration with the atmosphere at 25 °C during the Holocene and at 23 °C during the glacial interval<sup>10</sup>, regression of  $\epsilon_P$  on  $\log c$  for the points at 2.9, 8.5, 26.7, 33.9, 46.2, 60.1, 80.2 and 91.8 kyr BP yields  $a = -32.9$ ,  $b = 14.3$  (the calibration data are points for which stratigraphic uncertainties correspond to Vostok  $p_{CO_2}$  ranges of  $\leq 20$   $\mu\text{atm}$ ). Using these constants to calculate dissolved  $CO_2$  concentrations corresponding to each  $\epsilon_P$  value, and converting the concentrations to equilibrium  $p_{CO_2}$  values, the isotopically derived  $p_{CO_2}$  record shown in Fig. 2a is obtained. The Vostok ice-core  $p_{CO_2}$  record is shown for comparison. The  $p_{CO_2}$  records both demonstrate the sawtooth pattern typical of glacial-interglacial palaeochemical records<sup>22</sup>. Although misfits between the isotope and ice-core  $p_{CO_2}$  records are apparent and will be discussed below, the good correspondence strongly suggests that the isotope record contains information about  $CO_2$  levels.

Assumptions about the equilibration between the oceans and the atmosphere can be decreased using a second approach. Data reported by McCabe<sup>4</sup> and Rau *et al.*<sup>5</sup> for mixed lacustrine and marine phytoplanktonic communities, respectively, yield slopes ( $a$ ) of  $-17$  and  $-21$ . If we use  $a = -20$  as an intermediate value (favouring the marine system), the range of  $CO_2$  levels indicated by the isotope data exceeds that indicated by the ice core. This may be due to depletion of  $CO_2$  in surface waters during the glacial period or to the presence of excess  $CO_2$  in surface waters during the interglacial. The first alternative is consistent with suggestions that fertility of surface waters was enhanced during glacial intervals and with the observation that the net rate of accumulation of marine organic carbon during isotope stage 2 was  $1.8 \pm 1.0$  times higher than that during isotope stage 1<sup>15</sup>. Accordingly, we can choose  $b$  to reflect an approach to equilibrium only during interglacial periods. If values of  $c$  are calculated from all observations of  $\epsilon_P$  using  $a = -20$  and  $b = 2.5$ , the dissolved  $CO_2$  record shown in Fig. 2b is obtained. Also shown are the dissolved  $CO_2$  concentrations that would be expected if surface ocean water were in equilibrium with Vostok  $CO_2$  levels. Concentrations of dissolved  $CO_2$  inferred during the last glacial period are low in comparison with those expected on the basis of ocean-atmosphere equilibration (for example, 5.3 compared

with  $6.4 \mu\text{M}$  at 33.9 kyr, and 6.1 compared with  $6.8 \mu\text{M}$  at 80.2 kyr). The indicated disequilibria correspond to  $\Delta p_{\text{CO}_2}$  values of 20–40  $\mu\text{atm}$ , well within the range observed in modern oceans<sup>21</sup>.

Similar features appear in the sedimentary and ice-core records during the interval 50–90 kyr BP. Both, for example, indicate  $\text{CO}_2$  maxima near 68 kyr BP, but these maxima and other points of similarity between the records are not temporally coincident. Given the oxygen isotope record in the sediment core<sup>14</sup> and uncertainties regarding linear interpolation between stage boundaries<sup>15</sup>, it is possible, if not likely, that many of the misfits between the records reflect stratigraphic uncertainties.

The use of an isotope biomarker derived from a primary producer may be important in the recovery of the  $\text{CO}_2$ -related signal. A  $p_{\text{CO}_2}$  record based on the isotope difference between dissolved  $\text{CO}_2$  and total organic carbon (TOC) is shown in Fig. 2c. The curve is incongruent with the Vostok record of  $p_{\text{CO}_2}$  primarily because the isotopic composition of TOC has been strongly influenced by terrestrial contributions during the glacial intervals<sup>15,23</sup>. This calculation illustrates the potential problem

of deriving  $p_{\text{CO}_2}$  values from sedimentary organic carbon of mixed origins. There are other cases in which the isotope relationship between marine primary material and TOC has been affected by secondary processes, and in which correct calibration of an  $\epsilon$ - $c$  relationship would be impossible without resolution of the primary material<sup>8</sup>. Selection of the alkenones as primary biomarkers instead of tetrahydropyroles may have significant advantages. By focusing on a more restricted and uniform group of photosynthetic organisms, we may have avoided some ambiguities associated with varying biological responses to changes in  $p_{\text{CO}_2}$ . Coccolithophorids apparently lack a mechanism for accumulation of  $\text{CO}_2$  (ref. 24), making them particularly suitable as recorders of  $\text{CO}_2$  levels. Both coccoliths and their alkenone products are preserved in marine sediments, have existed since the Cretaceous<sup>25</sup>, and are widely distributed geographically<sup>26</sup>.

Our analyses of alkenones have allowed determination of the glacial-to-interglacial variation in the isotopic composition of the total biomass of the source organism<sup>3</sup> and the recovery of a  $\text{CO}_2$ -related signal covering ~100 kyr. This approach complements that of Broecker<sup>27</sup> and Shackleton *et al.*<sup>28</sup> who have shown that carbon isotope differences between benthic and planktonic foraminiferal carbonates can be interpreted in terms of total concentrations of dissolved inorganic carbon. Combining these and vertical nutrient distribution<sup>2</sup> approaches for the study of  $\text{CO}_2$  in ancient oceans should allow exploration of the redistribution of carbon in the ocean and of mechanisms controlling atmospheric  $p_{\text{CO}_2}$ . The question unresolved here, whether low  $c$  values during the glacial interval accurately reflect depletion of  $\text{CO}_2$  in the photic zone by carbon-fixing organisms, can be addressed by comparison of  $\text{CO}_2$  records from oceans with varying histories of biological productivity. In the same way, areas of  $\text{CO}_2$  uptake and release in ancient oceans may be detected. Derivation of a  $\text{CO}_2$ -related record from marine sediments should be useful in developing a longer-term (from ~100 kyr to as much as 200 Myr) understanding of natural processes affecting atmospheric  $p_{\text{CO}_2}$ . □

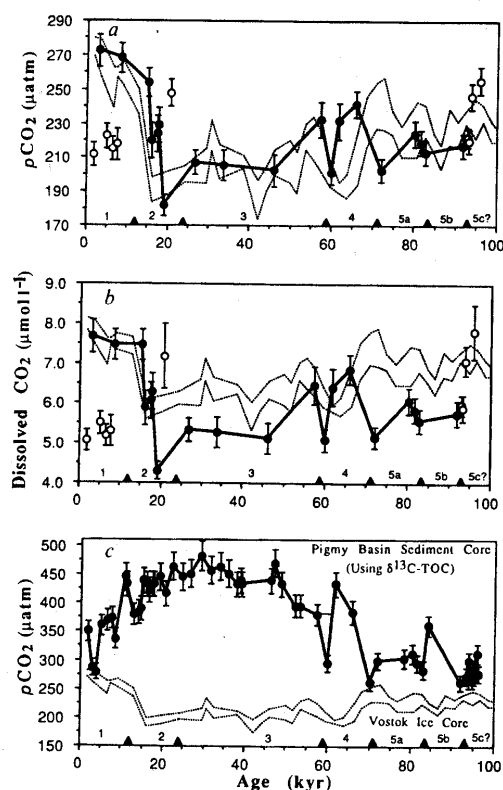


FIG. 2 a, Record of equilibrium atmospheric  $p_{\text{CO}_2}$  (see text) based on concentrations of dissolved  $\text{CO}_2$  calculated using equation (1) with  $a = -32.9$ ,  $b = 14.3$  and  $\epsilon_p$  values from Fig. 1c. The envelope (mean  $\pm 2\sigma$ ) of the atmospheric  $\text{CO}_2$  levels measured in the Vostok ice core<sup>1</sup> (dotted lines) is shown for comparison. b, Isotopically based record of sea surface concentrations of dissolved  $\text{CO}_2$  (see text) compared with a hypothetical record (dotted lines) derived from the Vostok results based on assumption of ocean-atmosphere equilibration (see text). c,  $p_{\text{CO}_2}$  record based on assumption that  $\delta_p = \delta_{\text{TOC}}$  ( $\delta_{\text{TOC}}$  values from ref. 15). The Vostok ice core  $p_{\text{CO}_2}$  record<sup>1</sup> is shown for comparison.

Received 7 June; accepted 8 August 1990.

1. Barnola, J. M., Raynaud, D., Korotkevich, Y. S. & Lorius, L. *Nature* **329**, 408–414 (1987).
2. Boyle, E. A. *J. geophys. Res.* **93**, 15701–15714 (1988).
3. Popp, B. N., Takigiku, R., Hayes, J. M., Landa, J. W. & Baker, E. W. *Am. J. Sci.* **285**, 436–454 (1989).
4. McCabe, B. thesis, Univ. of Waikato (1985).
5. Rau, G. H., Takahashi, T. & DesMarais, D. J. *Nature* **341**, 516–518 (1989).
6. Fairbanks, R. G., Sverdrup, M., Free, R., Wiebe, P. H. & Be, A. W. H. *Nature* **296**, 841–844 (1982).
7. Berger, W. H., Killingley, J. S. & Vincent, E. *Oceanologica Acta* **1**, 203–216 (1978).
8. Hayes, J. M., Popp, B. N., Takigiku, R. & Johnson, R. *Geochim. cosmochim. Acta* **53**, 2961–2972 (1989).
9. Freeman, K. H., Hayes, J. M., Trendel, J. M. & Albrecht, P. *Nature* **343**, 254–256 (1990).
10. Jasper, J. P. & Gagosian, R. B. *Paleoceanography* **4**, 603–614 (1989).
11. Mariotti, A. T. *et al. Br. phycol. J.* **19**, 203–216 (1984).
12. Bouma, A. H. *Am. Ass. Petrol. Geol. Mem.* **34**, 567–581 (1983).
13. Bouma, A. H. *et al. Init. Rep. DSDP Leg 96*, 777–780 (1986).
14. Williams, D. F. & Kohl, B. *Init. Rep. DSDP Leg 96*, 671–676 (1986).
15. Jasper, J. P. & Gagosian, R. B. *Geochim. cosmochim. Acta* **54**, 1117–1132 (1990).
16. Broecker, W. S. *Geochim. cosmochim. Acta* **46**, 1689–1705 (1982).
17. Newman, J. W., Parker, P. L. & Behrens, E. W. *Geochim. cosmochim. Acta* **37**, 225–238 (1973).
18. Ewing, M., Ericson, D. B. & Heezen, B. C. in *Habitat of Oil* (ed. Weeks, L. G.) 995–1054 (Am. Ass. Petrol. Geol., Tulsa, 1958).
19. Kohl, B. *Init. Rep. DSDP Leg 96*, 657–670 (1986).
20. Lorius, C. *et al. Nature* **316**, 591–596 (1985).
21. Tans, P. P., Fung, I. Y. & Takahashi, T. *Science* **247**, 1431–1438 (1990).
22. Broecker, W. S. & van Donk, J. *Rev. Geophys. Space Phys.* **8**, 169–189 (1978).
23. Jasper, J. P. & Gagosian, R. B. *Nature* **342**, 60–62 (1989).
24. Steeman Nielsen, E. *Marine Photosynthesis* (Elsevier, Amsterdam, 1975).
25. Farrimond, P., Eglinton, G. & Brassell, S. C. in *Advances in Organic Geochemistry 1985* (eds Leythaeuser, D. & Rullkötter, J.) 897–903 (Pergamon, Oxford, 1985).
26. Okada, H. & McIntyre, A. *Microscopaeontology* **23**, 1–13 (1977).
27. Broecker, W. S. *Prog. Oceanogr.* **11**, 151–197 (1982).
28. Shackleton, N. J., Hall, M. A., Line, J. & Clegg, S. *Nature* **306**, 319–322 (1983).
29. de Leeuw, J. W., van der Meer, F. W. & Rijstma, W. I. C. in *Advances in Organic Geochemistry 1979* (eds Douglas, A. G. & Maxwell, J. R.) 211–217 (Pergamon, Oxford, 1980).
30. Redka, J. A. & Maxwell, J. R. *Tetrahedron Lett.* **29**, 2599–2600 (1988).
31. Constans, R. E. & Parker, P. E. *Init. Rep. DSDP Leg 96*, 601–630 (1986).
32. Ledbetter, M. T. *Init. Rep. DSDP Leg 96*, 685–688 (1986).

ACKNOWLEDGEMENTS. We thank the DSDP and ODP for providing samples for this research, L. P. Brzuzy, K. H. Freeman and J. T. Hayes for mass spectrometric assistance, D. J. Hollander and K. H. Freeman for reviews of drafts of this report, and F. Prah and K. Amthor for providing a culture of *Emiliania huxleyi* and the related alkenone extract. This work was supported by the NSF.